TOXICOLOGICAL SCIENCES **125(1)**, 310–317 (2012)
doi:10.1093/toxsci/kfr223
Advance Access publication October 13, 2011

The Cutaneous Lesions of Dioxin Exposure: Lessons from the Poisoning of Victor Yushchenko

Jean-Hilaire Saurat,*,†,[1] Guerkan Kaya,*,† Nikolina Saxer-Sekulic,*,† Bruno Pardo,* Minerva Becker,‡ Lionel Fontao,† Florence Mottu,*,† Pierre Carraux,† Xuan-Cuong Pham,† Caroline Barde,† Fabienne Fontao,* Markus Zennegg,§ Peter Schmid,§ Olivier Schaad,¶ Patrick Descombes,¶ and Olivier Sorg*,†

*Swiss Centre for Applied Human Toxicology, Dermatotoxicology Unit, University of Geneva, 1211 Geneva 4, Switzerland; †Dermatology Department and ‡Radiology Department, Geneva University Hospital, 1211 Geneva 14, Switzerland; §EMPA (Swiss Federal Laboratories for Materials Testing and Research), 8600 Dübendorf, Switzerland; and ¶Genomics Platform, National Center of Competence in Research Frontiers in Genetics, University of Geneva, 1211 Geneva 4, Switzerland

[1]To whom correspondence should be addressed at Swiss Centre for Applied Human Toxicology, University of Geneva, 1, rue Michel-Servet, 1211 Genève 4, Switzerland. Fax: 0041-22-379 5502. E-mail: jean.saurat@unige.ch.

Received August 10, 2011; accepted August 10, 2011

Several million people are exposed to dioxin and dioxin-like compounds, primarily through food consumption. Skin lesions historically called "chloracne" are the most specific sign of abnormal dioxin exposure and classically used as a key marker in humans. We followed for 5 years a man who had been exposed to the most toxic dioxin, 2,3,7,8-tetrachlorodibenzo-*p*-dioxin (TCDD), at a single oral dose of 5 million-fold more than the accepted daily exposure in the general population. We adopted a molecular medicine approach, aimed at identifying appropriate therapy. Skin lesions, which progressively covered up to 40% of the body surface, were found to be hamartomas, which developed parallel to a complete and sustained involution of sebaceous glands, with concurrent transcriptomic alterations pointing to the inhibition of lipid metabolism and the involvement of bone morphogenetic proteins signaling. Hamartomas created a new compartment that concentrated TCDD up to 10-fold compared with serum and strongly expressed the TCDD-metabolizing enzyme cytochrome P450 1A1, thus representing a potentially significant source of enzymatic activity, which may add to the xenobiotic metabolism potential of the classical organs such as the liver. This historical case provides a unique set of data on the human tissue response to dioxin for the identification of new markers of exposure in human populations. The herein discovered adaptive cutaneous response to TCDD also points to the potential role of the skin in the metabolism of food xenobiotics.

Key Words: **dioxin; toxicity; skin; hamartoma; morphology.**

Dioxin (2,3,7,8-tetrachlorodibenzo-*p*-dioxin, TCDD) is the most potent of a large number of industrial-era halogenated polyaromatic hydrocarbon pollutants, including other dibenzo-*p*-dioxins, dibenzofurans, and certain polychlorinated biphenyls.

Human populations are exposed to low levels of dioxin and dioxin-like compounds, primarily through food consumption (Connor *et al.*, 2008; Schecter *et al.*, 1999). The risk characterization of dioxin exposure remains difficult to establish, although it is an issue that broadly affects important public health policy decisions (Gies *et al.*, 2007; Steenland *et al.*, 2001). Thus, chronic exposure to low/moderate doses of dioxin may be involved not only in the classic dioxin toxicity in some genetically predisposed individuals (IARC Monograph, 1997; Aylward *et al.*, 2005) but also in the newly identified role of these compounds in autoimmunity (Brembilla *et al.*, 2011; Marshall and Kerkvliet, 2010; Ramirez *et al.*, 2010).

In humans, skin lesions called "chloracne" are the most visible and consistent response to dioxin exposure and therefore play the role of a sentinel sign for toxicity (Caputo *et al.*, 1988). The mechanism by which chloracne appears was not previously known and its diagnostic value is not straightforward, especially in mild and sporadic cases, which could still relate to significant exposure (Passarini *et al.*, 2010). A robust indicator that would trigger specific ecotoxicology diagnostic processes is lacking; in the current situation, it is likely that many cases have not been recognized (Saurat and Sorg, 2010).

We have previously reported on the TCDD poisoning in Victor Yushchenko with identification and measurement of TCDD metabolites (Sorg *et al.*, 2009). The maximum accepted daily dose exposure in human is 4 pg/kg, and this patient received a single dose of 20 μg/kg.

With the approval of the patient to release peer-reviewed scientific information on his case, we now report on a set of data that has never been obtained in humans and helps define the phenotype of the dioxin-induced skin pathology.

MATERIALS AND METHODS

Clinical specimens. Skin sampling was performed under general anesthesia during therapeutic procedures.

Histopathological and immunohistochemical evaluation. Sections were cut from formalin-fixed, paraffin-embedded skin biopsy specimens and stained with hematoxylin and eosin. Cytochrome P450 (CYP) 1A1 immunohistochemical analysis was performed with the use of an immunoperoxidase technique according to standard procedures (Lebeau *et al.*, 2005).

Dioxin analysis. TCDD was determined in lipid extracts from serum and skin samples using gas chromatography with high-resolution mass spectrometry as previously described (Sorg *et al.*, 2009).

Imaging and volumetric analysis. Radiologic follow-up included high-resolution magnetic resonance (MR) imaging examinations of the face and head at 1.5 T and total body positron emission tomography/computed tomography (PET/CT) exams. The acquired MR and PET/CT data obtained for diagnostic, pretherapeutic, and follow-up purposes formed the basis of our volumetric analysis. The total skin volume and the combined volume of all hamartomatous skin lesions in the examined area were calculated separately using commercially available software according to the manufacturers' instructions (GE Healthcare Advantage Windows). Individual skin lesions on each slice were defined by manual contouring, and appropriate thresholding was used to determine total skin volume. The software was used to generate three-dimensional representations of the calculated total skin volume and of the calculated volume of all hamartomatous lesions.

Gene expression analysis. Total RNA extracts from skin samples (face) of the patient and four healthy Caucasian men matched for age, sex, race, and site of sampling were prepared as previously reported (Sorg *et al.*, 2008). RNA quality was assessed using an Agilent 2100 Bioanalyzer with an RNA 6000 Nano LabChip kit. We generated a hybridization mixture containing 15 µg of biotinylated complementary RNA and hybridized it to GeneChip HG U133 Plus 2.0 according to manufacturer's instructions (Affymetrix). To identify differentially expressed transcripts, comparisons were carried out after normalization with the Affymetrix GCOS 1.2 (MAS5) software.

Bioinformatic analysis. Responsive elements for genes corresponding to differentially expressed transcripts were searched with the University of California—Santa Cruz Genome Browser (http://genome.ucsc.edu/, March 2006 [NCBI36/hg18] assembly) in the Transcription Factor Binding Sites Conserved Track (Fujita *et al.*, 2010) and Gene2Promoter and MatInspector from Genomatix software (www.genomatix.de) (Cartharius *et al.*, 2005). For most of the tested genes, the same responsive elements were found with both resources.

RESULTS

Dioxin-Induced Skin Lesions Progress over Months while Internal Organs Heal

A few hours after dinner in Kiev on 5 September 2004, a 50-year-old male patient suddenly became severely ill. Hospital work-up revealed gastritis, colitis with multiple ulcers, hepatitis, and pancreatitis, all compatible with poisoning by an "unknown substance" because testing for thallium, arsenic, antimony, mercury, and lead was negative (Ryan, 2011). Severe facial edema appeared 2 weeks after the poisoning (W2 a.p.). By W6 a.p., the digestive tract symptoms had improved (Fig. 1). However, severe bilateral lower limb neuropathic pain appeared, and electroneuromyography confirmed that this was caused by small fiber peripheral neuropathy (The organs and systems involved, other than the skin, are just cited here. Each will be fully addressed in future publications when the mechanism has been better analyzed by appropriate ongoing data analysis.). Facial involvement worsened with diffuse nodular lesions on an edematous background, sparing of the periocular zone, but major involvement of the ears and retroauricular folds (Figs. 2A and 2B). The basic skin lesions were small nodules (Fig. 2C),

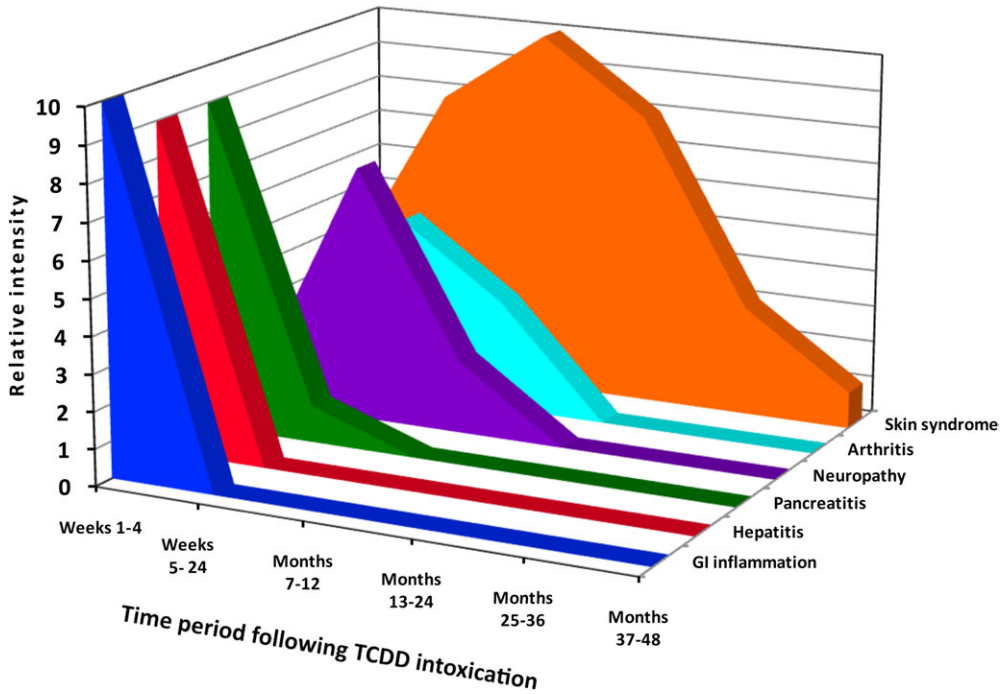

FIG. 1. Evolution of the dioxin disease. Chronology of organ involvement a.p. The peak of skin involvement is delayed as compared with the other organs, and skin lesions show a longer and chronic course.

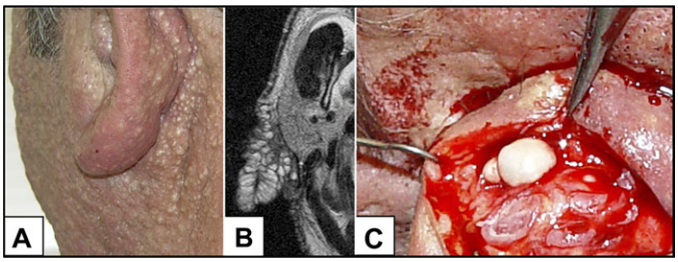

FIG. 2. Representative pictures of the skin lesions. (A) Facial, auricular, and retroauricular nodular lesions on an edematous background at month 4 a.p. (B) Axial, high-resolution T2-weighted MR image at the level of the mid face showing many hamartomas located in the dermis, on the cheek, the ear lobe, and retroauricular fold. Note variable size of the cysts, the largest being located in the ear lobe. Some cysts extend into the subcutaneous fat. (C) Per-operative aspect of the hamartomas on the ear lobule at month 4 a.p.

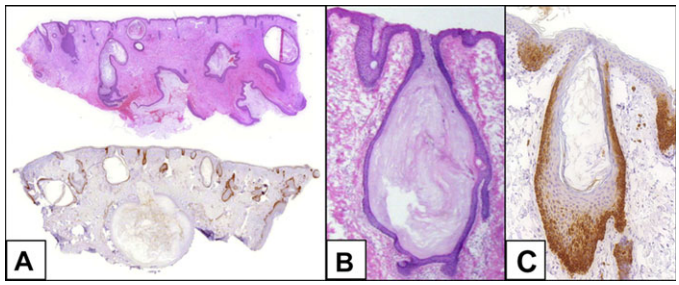

FIG. 3. Histological analyses of the skin lesions. (A) Photomicrograph of a skin sample from the retroauricular area stained with hematoxylin-eosin (upper part) showing the dermal distribution of the hamartomas and the absence of sebaceous glands and (lower part) reacted with anti-CYP1A1 showing the focal expression of the enzyme in the hamartomas (scanning magnification; monoclonal anti-CYP1A1 antibody, Santa Cruz Biotechnology, diluted 1:50). (B) Photomicrograph of one of the hamartoma showing mantle-like columnar epithelial downgrowths (Hematoxylin-eosin, original magnification: X20). (C) Immunohistochemical staining of CYP1A1 in a hamartoma. Original magnification: X20.

with rapid growth into cysts that developed severe painful inflammation. These lesions were clinically very similar to those of severe nodulocystic acne (Plewig and Kligman, 1993). By W10 a.p., a few scattered cystic lesions had appeared on the body, but it was not until 9 months (M9) a.p. that lesions became widespread over the entire body, including the limbs, with a peak clinical manifestation at M11 a.p (Fig. 1). Palms and soles were spared and have remained so for the subsequent years of follow-up. Only a few lesions occurred in the axillary and inguino genital folds.

Skin Lesions Are Hamartomas

The data are based on 52 skin specimens taken over M43, which showed consistently identical aspects. The key features were "structure loss" and "structure gain," with preservation of other normal skin structures, thereby compatible with hamartomas (http://en.wikipedia.org/wiki/Hamartoma) (Albrecht, 1904).

The structure loss was the disappearance of the sebaceous glands. This loss occurred to a striking extent: on 252 histological slides studied, not a single sebaceous gland was observed (a very conservative estimate of normal numbers would be from 500 to 4500 sebaceous glands observed on 252 slides) (Montagna, 1963).

The structure gain was the appearance of cystic lesions with epithelial walls showing epidermal-like differentiation with the expected distribution of epidermal keratins (not shown). These lesions (Figs. 3A–C) were either superficial with an open comedo-like aspect or extending much deeper in the dermis, hence resembling infundibular cysts (Plewig and Kligman, 1993), but with the following distinct characteristics: (1) mantle-like columnar epithelial downgrowths, showing high proliferative activity (Ki67-positive cells, not shown), putatively giving birth to new cysts, resulting in branching cystic figures with downward growth (Figs. 3A–C) and (2) focal expression of CYP1A1, the major dioxin-metabolizing CYP enzyme, in the epithelial walls of the cystic lesions as shown by immunohistochemistry (Figs. 3A and 3C).

Gene Expression in the Skin

Gene expression as monitored by whole-genome microarrays analysis was strongly altered in this hamartomatous skin, as compared with age, sex, race, and site of sampling skin specimens taken in healthy subjects (Table 1).

The majority of differentially expressed genes were repressed: thus, when a cutoff of more than twofold was considered for the analysis of skin samples taken at M5 a.p., 530 genes were found to be differentially expressed, 63% of which were repressed.

Table 1 shows a more stringent sorting, with only the genes downregulated more than 10-fold and those upregulated more than threefold in skin samples taken M5 a.p.. Table 1 includes in addition (1) the key genes of the aryl hydrocarbon receptor (AhR) dioxin signaling pathway, whatever their modulation, and (2) another transcriptome performed M11 a.p. in order to evaluate the permanence of the altered gene expression, which was found to be quite consistent (see Table 1, fold changes M5 and M11).

Among the genes known to be involved in AhR/dioxin pathway, the most induced were *CYP1A1, CYP1B1, CYP1A2*, and the aryl hydrocarbon receptor repressor (*AhRR*), whereas the *AhR* itself, its chaperones heat shock protein 90 and prostaglandin E synthase 3 (p23), as well as aryl hydrocarbon receptor nuclear translocator/*HIF*β genes were not differentially expressed. Real time PCR analysis for *AhR, AhRR, CYP1A1*, and CYP1A2, performed on independent samples dissected at the same time, confirmed these results (data not shown). This indicates that a strong and sustained induction of the AhR pathway does occur in the skin lesions and provides, for the first time in humans, information on the relative expression of each player under high dioxin exposure.

The most represented structural/functional family of genes differentially expressed was related to lipid metabolism. In this family, all genes were repressed except phospholipase A2 group IIA, which was induced threefold. The repressed genes

TABLE 1
Fold Changes of the Patient Compared with Means of Controls in Whole-Genome Microarray Gene Expression Analysis of Skin Samples of the Face Taken at Months 5 and 11 a.p. in (1) Genes of the Dioxin Signaling Pathway, (2) Genes Downregulated More than 10-fold, and (3) Genes Upregulated More than Threefold

				Fold change	
Structural/functional family	Affymetrix ID	Symbol	Description	5 months	11 months
Dioxin signaling pathway	205749_at	CYP1A1	Cytochrome P450, family 1, subfamily A, polypeptide 1	171.9	114.3
	202436_s_at	CYP1B1	Cytochrome P450, family 1, subfamily B, polypeptide 1	9.8	4.7
	207608_x_at	CYP1A2	Cytochrome P450, family 1, subfamily A, polypeptide 2	6.7	3.5
	229354_at	AhRR	Aryl hydrocarbon receptor repressor	3.9	4.2
	230619_at	ARNT	Aryl hydrocarbon receptor nuclear translocator	1.1	1.3
	200599_s_at	HSP90B1	Heat shock protein 90 kDa beta (Grp94), member 1	1.1	0.7
	201782_s_at	AIP	Aryl hydrocarbon receptor interacting protein	1.0	0.8
	200627_at	PTGES3	Prostaglandin E synthase 3 (cytosolic)	0.9	0.6
	202820_at	AhR	Aryl hydrocarbon receptor	0.8	0.9
Lipid metabolism	203649_s_at	PLA2G2A	Phospholipase A2, group IIA	3.1	1.9
	219429_at	FA2H	Fatty acid 2-hydroxylase	−4.9	−24.7
	210452_x_at	CYP4F2	Cytochrome P450, family 4, subfamily F, polypeptide 2	−6.5	−8.8
	205822_s_at	HMGCS1	3-Hydroxy-3-methylglutaryl-CoA synthase 1	−8.8	−20.8
	219131_at	UBIAD1	UbiA prenyltransferase domain containing 1	−10.5	−17.0
	221561_at	SOAT1	Sterol *O*-acyltransferase 1	−11.0	−45.9
	205404_at	HSD11B1	Hydroxysteroid (11-beta) dehydrogenase 1	−13.7	−17.4
	206465_at	ACSBG1	Acyl-CoA synthetase bubblegum family member 1	−15.8	−19.3
	221142_s_at	PECR	Peroxisomal trans-2-enoyl-CoA reductase	−16.1	−28.1
	232428_at	MOGAT2	Monoacylglycerol *O*-acyltransferase 2	−22.0	−107.1
	208962_s_at	FADS1	Fatty acid desaturase 1	−29.0	−33.4
	234513_at	ELOVL3	Elongation of very long chain fatty acids-like 3	−34.5	−110.7
	239108_at	FAR2	Fatty acyl CoA reductase 2	−38.4	−45.8
	205029_s_at	FABP7	Fatty acid–binding protein 7	−43.2	−6.8
	1553062_at	MOGAT1	Monoacylglycerol *O*-acyltransferase 1	−46.1	−165.3
	233126_s_at	OLAH	Oleoyl-ACP hydrolase	−54.0	−75.9
	210576_at	CYP4F8	Cytochrome P450, family 4, subfamily F, polypeptide 8	−66.7	−352.2
	1555416_a_at	ALOX15B	Arachidonate 15-lipoxygenase type I	−70.6	−1002.2
	205942_s_at	ACSM3	Acyl-CoA synthetase medium-chain family member 3	−75.0	−138.1
	1560507_at	AWAT1	Acyl-CoA wax alcohol acyltransferase 1	−79.4	−324.8
	202218_s_at	FADS2	Fatty acid desaturase 2	−114.9	−114.4
	204515_at	HSD3B1	Hydroxy-delta-5-steroid dehydrogenase, 3 beta- and steroid delta-isomerase 1	−129.9	−1066.0
	229476_s_at	THRSP	Thyroid hormone responsive	−2769.7	−250.1
Morphogenesis	240509_s_at	GREM2	Gremlin 2	6.3	2.2
	229404_at	TWIST2	Twist homolog 2	3.2	1.9
	226944_at	HTRA3	High temperature requirement factor A serine peptidase 3	3.2	1.3

TABLE 1—*Continued*

Structural/functional family	Affymetrix ID	Symbol	Description	Fold change 5 months	Fold change 11 months
Extracellular matrix	206026_s_at	TNFAIP6	Tumor necrosis factor alpha-induced protein 6	5.2	2.4
	202998_s_at	LOXL2	Lysyl oxidase-like 2	4.2	1.6
	206093_x_at	TNXB	Tenascin X	4.1	2.0
	202888_s_at	ANPEP	Alanyl (membrane) aminopeptidase	3.5	1.3
	209758_s_at	MFAP5	Microfibrillar associated protein 5	3.5	1.4
	202766_s_at	FBN1	Fibrillin 1	3.3	1.8
	220783_at	MMP27	Matrix metallopeptidase 27	3.1	1.5
	203184_at	FBN2	Fibrillin 2	3.1	3.7
	221731_x_at	VCAN	Versican	3.1	2.1
Inflammation	219837_s_at	CYTL1	Cytokine-like 1	5.9	6.2
	220351_at	CCRL1	Chemokine (C-C motif) receptor-like 1	4.1	3.0
	220088_at	C5AR1	Complement component 5a receptor 1	3.5	2.2
	213716_s_at	SECTM1	Secreted and transmembrane 1	3.1	3.0
Solute carrier family	225491_at	SLC1A2	Solute carrier family 1	3.2	1.7
	220435_at	SLC30A10	Solute carrier family 30, member 10	−10.3	−144.7
	223605_at	SLC25A18	Solute carrier family 25 (mitochondrial carrier), member 18	−11.2	−6.4
	205769_at	SLC27A2	Solute carrier family 27 (fatty acid transporter), member A2	−13.7	−9.3
	222071_s_at	SLCO4C1	Solute carrier organic anion transporter family, member 4C1	−20.2	−11.6
	205380_at	PDZK1	PDZ domain containing 1	−40.5	−131.4
	206143_at	SLC26A3	Solute carrier family 26, member 3	−59.3	−30.7
Various enzymes	206561_s_at	AKR1B10	Aldo-keto reductase family 1, member B10	4.3	2.0
	1555745_a_at	LYZ	Lysozyme	3.1	2.2
	206209_s_at	CA4	Carbonic anhydrase IV	3.1	2.0
	209522_s_at	CRAT	Carnitine acetyltransferase	−12.1	−11.7
	227055_at	METTL7B	Methyltransferase like 7B	−13.5	−7.6
	208383_s_at	PCK1	Phosphoenolpyruvate carboxykinase 1	−14.3	−9.1
	204836_at	GLDC	Glycine dehydrogenase	−27.6	−50.9
	220801_s_at	HAO2	Hydroxyacid oxidase 2	−30.6	−58.5
	205221_at	HGD	Homogentisate 1,2-dioxygenase	−38.5	−11.5
	220507_s_at	UPB1	Ureidopropionase, beta	−69.7	−133.8
	204997_at	GPD1	Glycerol-3-phosphate dehydrogenase 1	−86.2	−157.8
	239929_at	PM20D1	Peptidase M20 domain containing 1	−136.7	−128.1
Miscellaneous	205513_at	TCN1	Transcobalamin	21.9	1.8
	1562337_at	OR7D2	Olfactory receptor, family 7, subfamily D, member 2	5.2	5.1
	228335_at	CLDN11	Claudin 11	5.2	3.1
	220784_s_at	UTS2	Urotensin 2	4.9	14.9
	239492_at	SEC14L4	SEC14-like 4	−10.2	−12.6
	203001_s_at	STMN2	Stathmin-like 2	−13.9	−10.6
	201625_s_at	INSIG1	Insulin-induced gene 1	−16.6	−21.2
	213780_at	TCHH	Trichohyalin	−16.7	−1.8
	214624_at	UPK1A	Uroplakin 1A	−18.7	−99.7
	229095_s_at	LIMS3	LIM and senescent cell antigen-like domains 3-like	−27.2	−51.5
	210419_at	BARX2	BARX homeobox	−29.8	−2.7
	203400_s_at	TF	Transferrin	−74.4	−57.8
	214240_at	GAL	Galanin prepropeptide	−105.3	−473.3
	233052_at	DNAH8	Dynein, axonemal, heavy chain	−142.6	−153.7

Note. Microarray Database: http://www.ebi.ac.uk/arrayexpress/. Experiment Name: Dupond: Transcriptional Analysis of a Clinical Case of Acute Dioxin Poisoning; ArrayExpress Accession: E-MTAB-617. Reviewer's User Account—Username: Reviewer_E-MTAB-617, Password: ehhary9g.

included some genes specifically involved in sebum lipid metabolism.

AhR-responsive elements were identified in the promoter regions of *FADS2, AWAT1, ELOVL3, ALOX15B,* and sterol *O*-acyltransferase 1 genes.

The differentially expressed genes involved in tissue renewing may relate to hamartomas formation. Among the induced genes, gremlin 2 and high temperature requirement factor A serine peptidase 3, which encode for antagonists of the bone morphogenic protein family (BMP), may be highly relevant to the process of hamartomas formation (Sneddon *et al.*, 2006).

Most of the differentially expressed genes from structural/functional families shown in Table 1 as "extracellular matrix" and "inflammation" were induced, which was expected from the clinicopathological but does not suggest a specific pattern.

The solute carrier family genes were all strongly repressed except one. This family encodes proteins involved in the trafficking of many compounds including fatty acids, cholesterol, conjugated steroids, eicosanoids, peptides, and numerous drugs. That so many genes of this family/function were repressed suggests that specific studies are indicated for analyzing the link with dioxin toxicity. This also applies to the differentially expressed genes in the functional family of metabolism.

Dioxin Concentrates in the Skin Lesions: The Emergence of a New Compartment

Figure 4 shows the progressive decrease of TCDD levels in the serum, which contrasts with an increase of TCDD levels in the skin lesions that reaches a peak at M11 a.p. At that time, TCDD concentration in skin lesions was 10-fold that of serum. This indicates that the skin lesions do constitute a significant novel compartment, which we calculated to be for the face 482 cm^3 or 68.5% of the total skin volume (704 cm^3) (Fig. 5). Because at M11 a.p. 40% of the total body skin surface was covered with hamartomatous lesions, it can be estimated that during the peak manifestation of the cutaneous disease, the total volume of the hamartomatous compartment could have reached 6400 cm^3 for the entire body, containing about 35 µg TCDD, i.e., 2% of the initial total body burden.

Synopsis of Therapeutical Measures Derived from Observations

We initially observed that any incisional approach resulted in dystrophic healing, which we found to be a dioxin-induced, very fast skin healing response (Barouti *et al.*, 2009). With this important limiting feature to incisional skin intervention, we found that mechanical dermabrasion and multiple micro punch extraction/aspiration techniques yielded very quick healing (again due to the mechanism cited above) and were cosmetically still satisfactory. These methods allowed both significant pain relief from inflammation and extraction of large amounts of dioxin-rich hamartomatous lesions. A total of 26 procedures were performed on the whole-body skin surface under general anesthesia, from M4 to M46 a.p.

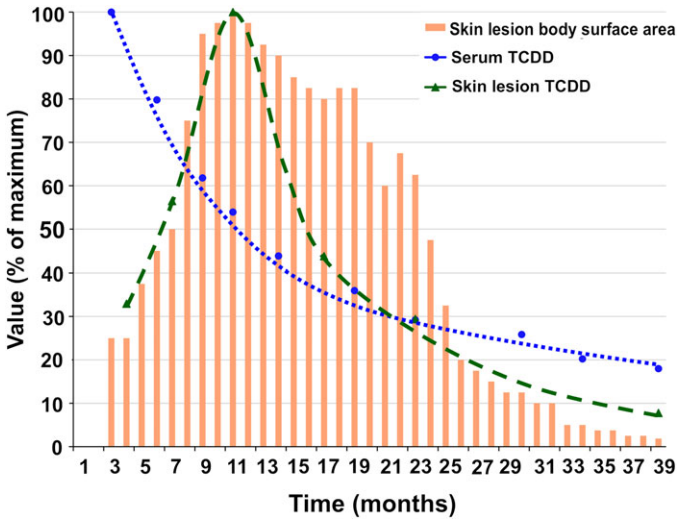

FIG. 4. Kinetics of TCDD showing the concentration of dioxin in the skin lesions: the emergence of a new compartment. Despite a progressive decrease in serum TCDD from months 3 to 15 a.p., there was a concomitant increase of TCDD concentration in skin, while the surface of skin involvement spread. For each parameter, the results are expressed as the percentage of the maximum values reached during this period of observation. The maximum values were as follows: (A) for skin lesions: 40% of total body surface area at M11 a.p. (evaluated prospectively by the palm of the hand method; Agarwal and Sahu, 2010); (B) for TCDD in serum: 890 pg/g wet weight (ww) at M3 a.p.; (C) for TCDD in skin lesions: 5000 pg/g ww at M11 a.p. At that time, TCDD concentration in skin lesions was therefore 10-fold that of serum. This indicates that the skin lesions do constitute a significant novel compartment, which could have reached 6400 cm3 for the entire body by M11 a.p., containing about 35 lg TCDD, i.e., 2% of the total initial body burden (see Fig. 5 and discussion).

Compassionate use of tumor necrosis factor α (TNF-α) blockade was considered because non-steroidal anti-inflammatory drugs and systemic steroids were not effective. The patient received three infusions of infliximab but because of intolerance was then switched to adalimumab, which was given for M18 (M16th to M34th a.p.).

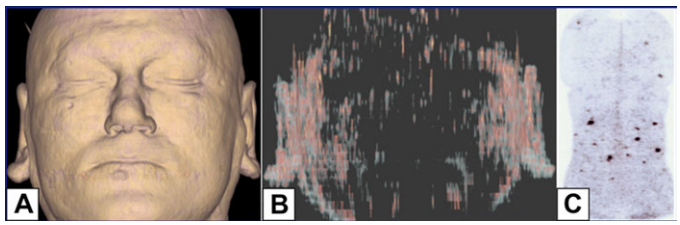

FIG. 5. Volumetric analyses of the skin lesions. (A) Three-dimensional representation of the calculated total skin volume of the face using the methodology described in the text. (B) Three-dimensional representation of the calculated volume of the hamartomatous lesions seen in the same area as in (A). Anterior view. Note that most lesions are located in the ear lobes and lateral cheeks. (C) Thick slab reconstruction of an FDG PET data set obtained from a whole-body PET/CT acquisition showing the distribution and the metabolism of the skin lesions on the back of the patient. Posterior view. Note that some lesions display a high metabolism (major FDG uptake, dark spots), whereas other lesions are metabolically less active (moderate FDG uptake, gray spots). "Metabolism" refers to FDG uptake, most probably linked to secondary inflammation rather than to CYP1A1/dioxin metabolism.

The M10 (M24th to M34th a.p.) during which adalimumab blood concentration was maintained at around 10 μg/ml (i.e., 80 mg every other week) corresponded to a progressive but very significant response on the inflammatory component. Generation of new hamartomatous lesions abruptly declined from month 28, but the extent to which this improvement was driven by TNF-α blockade versus the repeated interventional treatment is currently unclear. Moreover, we are aware that no conclusion may be extrapolated about therapeutic results from a single case.

DISCUSSION

This case being historically the one in whom the highest ever number of skin specimens have been obtained in a prospective context over four years, the data strongly support the previously proposed idea that sebaceous gland atrophy might be a major feature of dioxin toxicity (Panteleyev *et al.*, 1997; Suskind, 1985). In parallel to the observed atrophy of sebaceous glands, several genes encoding for key sebaceous lipid synthesis enzymes were strongly repressed. Because we identified AhR-responsive elements in the promoters of many of these genes, dioxin-induced transcriptional repression of lipid metabolism may be one mechanism driving the atrophy of sebaceous glands. This would also be consistent with the reported negative effect of AhR signaling in adipogenesis (Shimba *et al.*, 2003).

No specific characteristics had previously been shown to distinguish dioxin-induced skin lesions from those seen in nodulocystic acne or hidradenitis suppurativa (Plewig and Kligman, 1993). In this study, two distinct pathological signs were consistently identified in the patient's skin: one was a mantle-like outgrowth and the other a reproducible strong focal expression of CYP1A1 in the cyst cell wall. The "mantle" is thought to be an early stage in the formation of the sebaceous gland during the so-called sebaceous gland cycle (de Viragh, 1995). The ontogeny of the dioxin-induced hamartomas might therefore imply reprogramming of the sebaceous gland cycle, where sebaceous differentiation is replaced by a vigorous hamartomatous growth, driven by the dioxin-redistributed growth factors milieu. Transcriptomics in this case pointed to a very compatible pathway, the bone morphogenetic proteins and its antagonists: bone morphogenetic proteins are members of the transforming growth factor-beta family that has a role in proliferation, apoptosis, and differentiation in various tissues and organs, including skin. BMP signaling has been shown to be necessary for maintaining quiescence of adult epidermal stem cells, and it is likely that BMP signaling acts through other pathways in regulating quiescence and proliferation (Kangsamaksin and Morris, 2011; Sneddon *et al.*, 2006). This needs to be specifically explored, with appropriate experimental models, for deciphering the mechanisms of such morphogenetic properties of dioxin in skin and potentially in other organs.

The strong expression of CYP1A1 protein in the hamartoma cell wall but not in the adjacent skin epithelia, as detected by immunohistochemistry, matches the strong *CYP1A1* gene induction found in tissue. It appears to be a candidate new marker of dioxin-induced skin pathology; thus, the striking picture shown in Figure 3C (1) was seen in all biopsy specimens from the patient, (2) was absent in a panel of skin cysts including hidradenitis suppurativa (not shown), (3) was found in patients of a recent chloracne outbreak in Italy (Passarini *et al.*, 2010) (not shown), and more importantly (4) we could observe a sticking identical picture in archival skin specimens from the only previous human case with a similar high level of dioxin exposure, published by Geusau *et al.* (1999) (not shown, see acknowledgments).

In addition to its potential diagnostic interest, there are two further implications of the strong focal expression of CYP1A1 in the hamartomas.

First, the CYP1A1 may have role in the skin pathology. CYP1A1 expression has been correlated to TCDD toxicity in various *in vitro* and animal models (Rifkind, 2006). In particular, arachidonate, the gene pathway metabolism of which was associated to the most differently expressed in the skin of our patient, is a substrate for CYP1A1 and even more CYP1A2. Therefore, bioactive arachidonate derivatives could be involved in some TCDD effects (Rifkind, 2006).

Second, skin-expressed CYP1A1 may itself play a direct role in the phase I metabolism of dioxin, which we have recently characterized for the first time in humans (Sorg *et al.*, 2009). The amount of CYP1A1 protein available through a multitude of skin hamartomas represents a potentially significant source of enzymatic activity, which may add to the xenobiotic metabolism potential of the classical organs such as the liver.

The skin lesions historically called chloracne therefore represent a functional hamartomatous adaptive process to this poison exposure. We have suggested they would better be called "metabolizing acquired dioxin-induced skin hamartomas" (Saurat and Sorg, 2010). Such an adaptive response points to the potential role of the skin in the metabolism of orally introduced xenobiotics, other than dioxin, as well (Rowe *et al.*, 2008).

FUNDING

Swiss Center for Applied Human Toxicology and Dermatology Fund University of Geneva (UF1024).

ACKNOWLEDGMENTS

Marion Bonna is acknowledged for her invaluable contribution to the administrative management of the case. R. Fedosyuk, R. Valikhnovskyi, V. Kniazevych, O. Gaide, M. Harms, D. Salomon, A. Skaria, C. Tschanz, A. M. Thielen, and G. Marrazza are acknowledged for their most significant contribution to the medical team involved in the patient care. Many consultants from our institution, University Hospital of Geneva, Faculty of Medicine of Geneva, as well from other

countries around the world provided help and advice at all stages of the project; each will be specifically cited and acknowledged in further relevant publications. Alexandra Geusau, Vienna, is warmly acknowledged for providing skin specimens from her historical case for CYP1A1 staining. We thank M. Jorge Remunian for his valuable help with the volume calculations and Oliver Hartley for kindly reviewing the manuscript. Author contribution: J.H.S. and O.S. designed the study and wrote the manuscript; G.K., N.S., L.F., F.M., P.C., C.P., C.B., and F.F. performed and analyzed histological analyses; M.Z. and P.S. determined dioxin concentrations; and O.S. and P.D. performed genomic analyses. The authors have no competing interests to declare.

REFERENCES

Agarwal, P., and Sahu, S. (2010). Determination of hand and palm area as a ratio of body surface area in Indian population. *Indian J. Plast. Surg.* **43,** 49–53.

Albrecht, E. (1904). Über hamartome. *Dtsch. Ges. Pathol.* **7,** 153–157.

Aylward, L. L., Lamb, J. C., and Lewis, S. C. (2005). Issues in risk assessment for developmental effects of 2,3,7,8-tetrachlorodibenzo-p-dioxin and related compounds. *Toxicol. Sci.* **87,** 3–10.

Barouti, N., Fontao, L., Pardo, B., Sorg, O., and Saurat, J. H. (2009). AhR pathway as a novel pharmacological target for wound healing. *J. Invest. Dermatol.* **129,** S80.

Brembilla, N. C., Ramirez, J. M., Chicheportiche, R., Sorg, O., Saurat, J. H., and Chizzolini, C. (2011). In vivo dioxin favors interleukin-22 production by human CD4+ T cells in an aryl hydrocarbon receptor (AhR)-dependent manner. *PLoS One* **6,** e18741.

Caputo, R., Monti, M., Ermacora, E., Carminati, G., Gelmetti, C., Gianotti, R., Gianni, E., and Puccinelli, V. (1988). Cutaneous manifestations of tetrachlorodibenzo-p-dioxin in children and adolescents. Follow-up 10 years after the Seveso, Italy, accident. *J. Am. Acad. Dermatol.* **19,** 812–819.

Cartharius, K., Frech, K., Grote, K., Klocke, B., Haltmeier, M., Klingenhoff, A., Frisch, M., Bayerlein, M., and Werner, T. (2005). MatInspector and beyond: Promoter analysis based on transcription factor binding sites. *Bioinformatics* **21,** 2933–2942.

Connor, K. T., Harris, M. A., Edwards, M. R., Budinsky, R. A., Clark, G. C., Chu, A. C., Finley, B. L., and Rowlands, J. C. (2008). AH receptor agonist activity in human blood measured with a cell-based bioassay: Evidence for naturally occurring AH receptor ligands in vivo. *J. Expo. Sci. Environ. Epidemiol.* **18,** 369–380.

de Viragh, P. A. (1995). The 'mantle hair of Pinkus.' A review on the occasion of its centennial. *Dermatology* **191,** 82–87.

Fujita, P. A., Rhead, B., Zweig, A. S., Hinrichs, A. S., Karolchik, D., Cline, M. S., Goldman, M., Barber, G. P., Clawson, H., Coelho, A., *et al.* (2010). The UCSC Genome Browser database: Update 2011. *Nucleic Acids Res.* **39,** D876–D882.

Geusau, A., Tschachler, E., Meixner, M., Sandermann, S., Päpke, O., Wolf, C., Valic, E., Stingl, G., and McLachlan, M. (1999). Olestra increases faecal excretion of 2,3,7,8-tetrachlorodibenzo-p-dioxin. *Lancet* **354,** 1266–1267.

Gies, A., Neumeier, G., Rappolder, M., and Konietzka, R. (2007). Risk assessment of dioxins and dioxin-like PCBs in food—Comments by the German Federal Environmental Agency. *Chemosphere* **67,** S344–S349.

IARC Monograph on the Evaluation of Carcinogenic Risks to Humans. (1997). *Polychlorinated Dibenzo-Para-Dioxins and Polychlorinated Dibenzofurans*, pp. 33–343. IARC, Lyon, France.

Kangsamaksin, T., and Morris, R. J. (2011). Bone morphogenetic protein 5 regulates the number of keratinocyte stem cells from the skin of mice. *J. Invest. Dermatol.* **131,** 580–585.

Lebeau, S., Masouyé, I., Berti, M., Augsburger, E., Saurat, J. H., Borradori, L., and Fontao, L. (2005). Comparative analysis of the expression of ERBIN and Erb-B2 in normal human skin and cutaneous carcinomas. *Br. J. Dermatol.* **152,** 1248–1255.

Marshall, N. B., and Kerkvliet, N. I. (2010). Dioxin and immune regulation: Emerging role of aryl hydrocarbon receptor in the generation of regulatory T cells. *Ann. N. Y. Acad. Sci.* **1183,** 25–37.

Montagna, W. (1963). In *The Sebaceous Glands* (W. Montagna, R. A. Ellis and A.F. Silver, Eds.), pp. 167–187. Pergamon Press, Oxford, U.K.

Panteleyev, A. A., Thiel, R., Wanner, R., Zhang, J., Roumak, V. S., Paus, R., Neubert, D., Henz, B. M., and Rosenbach, T. (1997). 2,3,7,8-Tetrachlorodibenzo-p-dioxin (TCCD) affects keratin 1 and keratin 17 gene expression and differentially induces keratinization in hairless mouse skin. *J. Invest. Dermatol.* **108,** 330–335.

Passarini, B., Infusino, S. D., and Kasapi, E. (2010). Chloracne: Still cause for concern. *Dermatology* **221,** 63–70.

Plewig, G., and Kligman, A. M. (1993). In *Acne and Rosacea*. Springer-Verlag, Berlin, Germany.

Ramirez, J. M., Brembilla, N. C., Sorg, O., Chicheportiche, R., Matthes, T., Dayer, J. M., Saurat, J. H., Roosnek, E., and Chizzolini, C. (2010). Activation of the aryl hydrocarbon receptor reveals distinct requirements for IL-22 and IL-17 production by human T helper cells. *Eur. J. Immunol.* **40,** 2450–2459.

Rifkind, A. B. (2006). CYP1A in TCDD toxicity and in physiology—With particular reference to CYP dependent arachidonic acid metabolism and other endogenous substrates. *Drug Metab. Rev.* **38,** 291–335.

Rowe, J. M., Welsh, C., Pena, R. N., Wolf, C. R., Brown, K., and Whitelaw, C. B. (2008). Illuminating role of CYP1A1 in skin function. *J. Invest. Dermatol.* **128,** 1866–1868.

Ryan, J. J. (2011). In *The Yushchenko Dioxin Poisoning: Chronology and Pharmacokinetics*. Wiley, Hoboken, NJ.

Saurat, J. H., and Sorg, O. (2010). Chloracne, a misnomer and its implications. *Dermatology* **221,** 23–26.

Schecter, A. J., Sheu, S. U., Birnbaum, L. S., DeVito, M. J., Denison, M. S., and Päpke, O. (1999). A comparison and discussion of two different methods of measuring dioxin-like compounds: Gas chromatography–mass spectrometry and the CALUX bioassay F implications for health studies. *Organohal. Compounds* **40,** 247–250.

Shimba, S., Hayashi, M., Ohno, T., and Tezuka, M. (2003). Transcriptional regulation of the AhR gene during adipose differentiation. *Biol. Pharm. Bull.* **26,** 1266–1271.

Sneddon, J. B., Zhen, H. H., Montgomery, K., van de Rijn, M., Tward, A. D., West, R., Gladstone, H., Chang, H. Y., Morganroth, G. S., Oro, A. E., *et al.* (2006). Bone morphogenetic protein antagonist gremlin 1 is widely expressed by cancer-associated stromal cells and can promote tumor cell proliferation. *Proc. Natl. Acad. Sci. U.S.A.* **103,** 14842–14847.

Sorg, O., Tran, C., Carraux, P., Grand, D., Barraclough, C., Arrighi, J. F., Descombes, P., Piguet, V., and Saurat, J. H. (2008). Metabolism and biological activities of topical 4-oxoretinoids in mouse skin. *J. Invest. Dermatol.* **128,** 999–1008.

Sorg, O., Zennegg, M., Schmid, P., Fedosyuk, R., Valikhnovskyi, R., Gaide, O., Kniazevych, V., and Saurat, J. H. (2009). 2,3,7,8-Tetrachlorodibenzo-p-dioxin (TCDD) poisoning in Victor Yushchenko: Identification and measurement of TCDD metabolites. *Lancet* **374,** 1179–1185.

Steenland, K., Deddens, J., and Piacitelli, L. (2001). Risk assessment for 2,3,7,8-tetrachlorodibenzo-p-dioxin (TCDD) based on an epidemiologic study. *Am. J. Epidemiol.* **154,** 451–458.

Suskind, R. R. (1985). Chloracne, "the hallmark of dioxin intoxication." *Scand. J. Work Environ. Health* **11,** 165–171.